THE JOURNAL OF PHYSICAL CHEMISTRY A
A JOURNAL OF THE AMERICAN CHEMICAL SOCIETY

pubs.acs.org/JPCA Article

Proximity Effects of Substituents on Halogen Bond Strength

Jordan Lapp and Steve Scheiner*

Cite This: J. Phys. Chem. A 2021, 125, 5069–5077 Read Online

ACCESS | Metrics & More | Article Recommendations | Supporting Information

ABSTRACT: It is well known that the presence of an electron-withdrawing substituent (EWS) placed near the halogen (X) atom on a Lewis acid molecule amplifies the ability of this unit to engage in a halogen bond with a base. Quantum calculations are applied to examine how quickly these effects fade as the EWS is moved further and further from the X atom. Conjugated alkene and alkyne chains of varying lengths with a terminal C−I first facilitate analysis as to how the number of these multiple bonds affects the strength of CI··N XB to NH_3. Then, electron-withdrawing F and C≡N substituents are placed on the opposite end of the chain, and their effects on the XB properties are monitored as a function of their distance from I. These same EWSs are added to the ortho, meta, and para positions of aromatic iodobenzene. It is found that the XB grows in strength as more triple bonds are added to the alkyne, but there is little change caused by elongating an alkene. The cyano group has a much stronger effect than does F. While F strengthens the XB, its effects are quickly attenuated as it is moved further from I. The consequences of C≡N substitution are stronger and extend over a longer distance. Placement of an EWS on the phenyl ring diminishes with distance: *o* > *m* > *p*, and the effects of disubstitution are nearly additive. These trends apply not only to energetics but also to geometries, properties of the wave function, *σ*-hole depth, and NMR shielding.

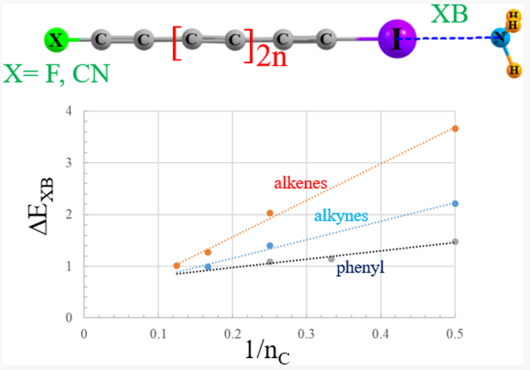

INTRODUCTION

Recent years have witnessed an explosive growth in the study of noncovalent bonds that are close parallels of the venerable H-bond. In each of the chalcogen, pnicogen, tetrel, and triel bonds, an atom of that same particular family of the periodic table replaces the bridging proton of the H-bond.[1−21] Among these interactions, the halogen bond (XB) is arguably the one that has been acknowledged for the longest time[22−27] and has engendered the greatest amount of scrutiny. Extensive study has demonstrated that the XB owes its stability to several factors.[28−37] In the first place, the electron-density cloud surrounding the X atom is quite anisotropic; while the overall charge on the X atom is partially negative, there is a pocket of positive potential that lies along the extension of the covalent C−X bond, which is commonly referred to as a *σ*-hole. This positive region attracts the negative potential of an approaching nucleophile, for example, its lone pair, leading to a Coulombic attraction. As a supplement, there is stabilizing charge transfer from the nucleophile lone pair into the *σ**(C−X) antibonding orbital, which is typically associated with C−X bond stretching. An additional factor is the ubiquitous attractive London dispersion energy, which contributes in varying amounts to different sorts of XBs.

Because of its ability to deepen the *σ*-hole on the X atom, as well as reduce the energy of the antibonding *σ** orbital that maximizes its stabilizing interaction with the lone pair orbital energy, the presence of an electron-withdrawing substituent (EWS) on the C atom to which the X atom is attached has been well established to strengthen the CX···Nuc halogen bond. It can be anticipated that the displacement of the EWS to another C atom, further away from X, would mitigate its effect. However, it is unclear how strong this mitigation might be. Would its effects be essentially eliminated if it is moved only one C away? If not, then, how quickly do these effects diminish as the EWS is moved away, and how far from X might these effects remain before fading completely?

These questions are examined here in the context of unsaturated carbon chains. It is thought that a series of conjugated double or triple bonds ought to best be able to convey the effects of an EWS along the chain, so the systems of this type are considered here. Alkenes and alkynes of varying lengths, containing a series of conjugated multiple bonds, are constructed, with a halogen atom on one end. Also of interest are halogen-substituted phenyl rings, which are very commonly involved in halogen bonds. Their aromatic character provides an interesting forum to consider the effects of an EWS in each of the various positions relative to the halogen atom, where it can exert not only an inductive effect but also modify the stability of various resonance structures of the ring.

Received: April 28, 2021
Published: June 3, 2021

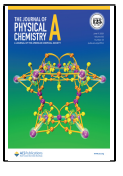

https://doi.org/10.1021/acs.jpca.1c03817
J. Phys. Chem. A 2021, 125, 5069−5077

SYSTEMS AND METHODS

Conjugated unsaturated hydrocarbon chains of varying lengths, both alkynes and alkenes, were constructed with an I atom on one end, for example, the 4-carbon units HC≡C-C≡C−I and H_2C═CH−CH═CHI. I was chosen as the halogen atom for consideration as it typically forms the strongest halogen bonds. These molecules place the I on a sp- and sp^2-hybridized C, respectively. In some cases, the electron-withdrawing F and C≡N substituents were placed on the opposite end of each chain, so their distance from I was determined by the chain length. Examples of these substituted units are displayed in Figure 1a and b. Note that two substituents were added to the

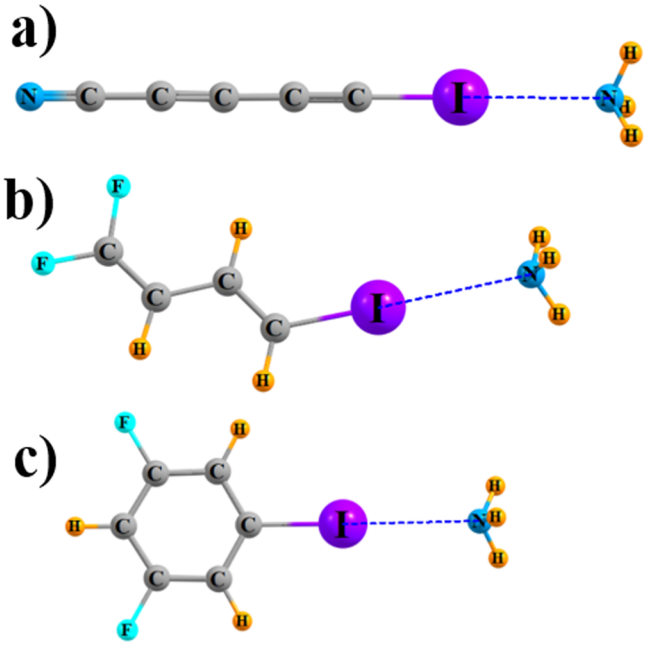

Figure 1. Molecular structures of representative halogen-bonded dimers of NH_3 with Lewis acids (a) NC−C≡C−C≡C−I, b) F_2C═CH-CH=CHI, and c) di-F-meta-substituted phenyl ring.

end of alkene chains and only one for alkynes. Another unsaturated system of interest is the I-substituted phenyl ring, which places the I on a sp^2-hybridized aromatic C. Substituents F and CN were added to this ring at various locations, ortho, meta, and para to the I. The meta-difluorinated ring is exhibited in Figure 1c as an example. A NH_3 molecule was used as the nucleophile that interacts through a XB with the σ-hole on the I atom, as shown in Figure 1. This unit was chosen for its moderate basicity, which is coupled with its small size that reduces the likelihood of complicating secondary interactions. As another advantage, NH_3 is very commonly used in this capacity in other studies of noncovalent bonds, facilitating comparisons with previous calculations.

All calculations were carried out in the framework of the Gaussian-09[38] package. The M06-2X DFT functional was applied in conjunction with the aug-cc-pVDZ basis set and with the fourth-row I atom represented by the aug-cc-pVDZ-PP relativistic pseudopotential from the EMSL library.[39,40] Numerous previous studies support the accuracy and dependability of this level of theory for related sorts of noncovalent interactions.[41−48] The geometries of all species were fully optimized and verified as true minima by the presence of only positive vibrational frequencies. Interaction energies E_{int} are defined as the difference between the energy of the complex and the sum of the two monomers of which it is comprised, holding their internal geometries as in the complex. E_{int} was corrected for the basis set superposition error using the counterpoise procedure.[49−51] The topology of the electron density was analyzed via the Atoms in Molecules (AIM)[52,53] treatment, via AIMAII.[54] Maxima on the ρ = 0.001 au isodensity surface of the molecular electrostatic potentials (MEPs) were located and evaluated with the Multiwfn program.[55] Nuclear magnetic resonance (NMR) chemical shielding was considered within the Gauge-Invariant Atomic Orbital (GIAO) context, again using the aug-cc-pVDZ basis set for all atoms except I, for which the all-electron Sapporo DKH3-DZP-2012 basis[56,57] was applied so as to capture the changes within the inner shells that lie close to the nucleus.

RESULTS

Several representative complexes are illustrated in Figure 1 to illuminate the nomenclature and the orientations. Full coordinates are provided for all such complexes as well as their optimized constituent monomers, and they are provided in the Supporting Information.

Energetics. The analysis begins with the energetics of dimerization. The interaction energies for each unsaturated iodinated system with NH_3 are displayed in the first column of Table 1. It is first evident that the alkynes form a stronger XB

Table 1. Interaction Energy ($-E_{int}$, Kcal/Mol) of XB between Indicated Lewis Acid and NH_3, and Differences between R-Substituted and Unsubstituted (R = H) Acids

	H	F	F−H	CN	CN−H
n	alkynes RC $-C_n-$CI				
0	6.95	7.47	0.52	9.16	2.21
2	7.56	7.49	−0.07	8.96	1.40
4	7.86	7.79	−0.07	8.85	0.99
	alkenes $R_2C-(CH)_n-CHI$				
0	3.61	5.42	1.81	7.27	3.66
2	3.72	4.01	0.29	5.75	2.03
4	3.70	3.77	0.07	4.97	1.27
6	3.70	3.76	0.06	4.71	1.01
	phenyl R-φ-I				
o	3.65[a]	4.46	0.81	5.13	1.48
m		4.17	0.52	4.79	1.14
p		4.01	0.36	4.74	1.09
o,o		5.34	1.69	6.64	2.99
m,m		4.70	1.05	5.93	2.28

[a]unsubstituted C_6H_5I

than the alkenes or aromatic systems. The interaction energies of the former lie in the 7−8 kcal/mol range, with smaller values of about 3.5 kcal/mol for the latter. With regard to the alkynes, adding additional C≡C bonds to the alkyne unit strengthen the XB, whereas there is little effect caused by increasing the number of double bonds in the alkenes.

The next column reports the XB energy when a F substituent is added to the terminus of each chain. There is a clear strengthening of the XB resulting from this substitution, as indicated by the succeeding F-H column, which lists the increase in interaction energy between the F-substituted and unsubstituted Lewis acid. Placing an F atom on the monoalkyne FC≡CI increases the interaction energy by 0.5 kcal/mol, but this effect is quickly damped as the chain grows

https://doi.org/10.1021/acs.jpca.1c03817
J. Phys. Chem. A 2021, 125, 5069−5077

longer. F-substitution exerts a stronger effect on the alkenes, in part due to the fact that there are two such F atoms added to the end of the chain. Such a replacement increases the interaction energy in the monoalkene by 50%, and there are even small residual effects as more double bonds are inserted between the F and I.

The lowermost section of Table 1 shows how the bond-strengthening effect of the F substituent on the aromatic ring drops as the F moves further away from the I, from ortho to meta to para. This sequence reduces XB strengthening from 0.81 to 0.52 to 0.36 kcal/mol. Disubstitution results in a doubling of the effect: Two ortho or meta F atoms increase bond strengthening by twice that of a single such replacement.

The last two columns of Table 1 reflect greater bond strengthening that results when the F substituent is replaced by the more electron-withdrawing C≡N. In the first place, the interaction energies are considerably larger, up to as much as 9 kcal/mol for the alkynes. Cyano substitution leads to interaction energy enhancements of as much as 3.66 kcal/mol. As in the F case, the alkenes are most affected by the substitution. Again, the effect of the substituent follows the $o > m > p$ sequence in the phenyl ring, and disubstitution doubles this effect. The tailing off of this magnification as the C≡N group is moved further away from the I is especially clear in the last column of Table 1. Note also that this bond strengthening persists even as the cyano group moves away from I by as much as eight C atoms.

In the study of cooperative effects, there is often found to be a good linear correlation[58,59] between the energetics and the reciprocal of the number of molecules within a chain. It is thus interesting to consider whether there is such a correlation here between the interaction energy and the reciprocal of the number of C atoms that intervene between the substituent and the I atom on the Lewis acid. Indeed, a very strong correlation was found here. The correlation coefficient R^2 is equal to 0.991 and 0.996 for the cyano substitution on the alkynes and alkenes, respectively, and slightly smaller 0.95 for the monosubstituted phenyl systems. The linear plots of these species are illustrated in Figure 2. The higher sensitivity of the

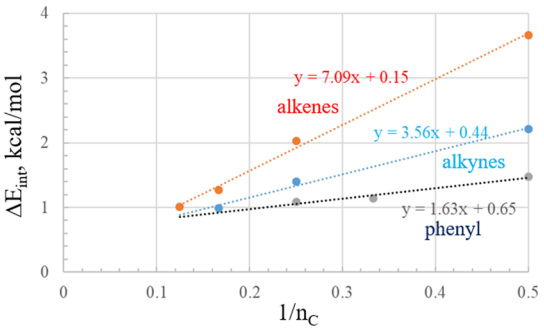

Figure 2. Relationship between the enhancement of interaction energies caused by cyano substitution and the reciprocal of the number of C atoms lying between the C≡N and I groups on Lewis acid

alkenes as compared to alkynes is reflected in the steeper slope of the former, by a factor of 2, with another drop by 2 for the phenyl system. The nonzero intercepts, albeit small ones, amplify the lingering effects of the cyano group even on a very long chain.

Geometry and Wave Function Analyses. One would expect that the noncovalent bond strengthening ought to be accompanied by a shortening of the intermolecular distance, particularly as the I and N atoms involved in the direct bonding remain the same throughout. The intermolecular bond distances are listed in Table 2, along with the changes

Table 2. Intermolecular R(I··N) (Å) Distance in Complex with NH_3

	H	F	F−H	CN	CN−H
n	alkynes RC−C_n−CI				
0	2.9520	2.9287	−0.0233	2.8860	−0.0660
2	2.9347	2.9369	0.0022	2.8923	−0.0424
4	2.9251	2.9279	0.0028	2.8945	−0.0306
	alkenes R_2C−$(CH)_n$−CHI				
0	3.1456	3.0238	−0.1218	2.9692	−0.1764
2	3.1410	3.1206	−0.0204	3.0357	−0.1053
4	3.1366	3.1329	−0.0037	3.0691	−0.0675
6	3.1320	3.1290	−0.0030	3.0793	−0.0527
	phenyl R-φ-I				
o	3.1384	3.0721	−0.0663	3.0336	−0.1048
m		3.0996	−0.0388	3.0644	−0.0740
p		3.1148	−0.0236	3.0771	−0.0613
o,o		3.0139	−0.1245	2.9637	−0.1747
m,m		3.0717	−0.0667	3.0145	−0.1239

occasioned by each F or C≡N substitution. These bond lengths are in the neighborhood of 3.0 Å and are slightly shorter for the sp-alkynes than the sp^2-alkenes or aromatics. The substitution of electron-withdrawing groups shortens these distances, which is consistent with their energetic strengthening. These bond contractions are largest for the disubstituted alkenes where they can be as large as 0.176 Å for $(CN)_2$−C═CHI. Also obeying the same trends as the energetics, the bond length reductions are magnified for C≡N vs F, and the effects drop as the substituent moves further away from the I along the chain. Note that this drop is a slow one, particularly for C≡N where it will persist for even longer chains than those considered here. Also consistent is that the ortho positioning is more effective than the meta or para positioning, and there is near doubling resulting from disubstitution.

There are several indicators of the strength of a noncovalent bond. One of the most prominent of these is the electron density at the bond critical point, within the AIM formalism for the analysis of the topology of the electron density. These densities may be seen from the first column of Table 3 to be on the order of 0.014 to 0.020 au for the unsubstituted Lewis acids, typical of halogen and other noncovalent bonds. The densities are larger for the sp-hybridized alkynes as compared to the alkenes and phenyl systems with their sp^2 hybridization. These quantities mirror the increasing interaction energies as more triple bonds are added to the acid, as well as the insensitivity to the number of double bonds in the alkenes. Also common to the energetics, the replacement of a terminal H atom by F or C≡N enhances ρ_{BCP}, much more so for C≡N than for F. Again, one sees a slow attenuation of the substituent effect as it is moved further from the I, whether alkyne, alkene, or aromatic.

As a supplementary means of evaluating halogen bond strength, one can consider the magnitude of the second-order perturbation theory energy E(2) for the transfer of charge from

https://doi.org/10.1021/acs.jpca.1c03817
J. Phys. Chem. A 2021, 125, 5069−5077

Table 3. Electron Density (10^{-4} au) at the I··N Bond Critical Point in Complexes with NH_3

	H	F	F−H	CN	CN−H
n	alkynes RC−C_n−CI				
0	194	202	8	221	27
2	201	200	−1	218	17
4	205	203	−2	217	12
	alkenes $R_2C-(CH)_n-CHI$				
0	140	172	32	193	53
2	141	147	6	171	30
4	143	143	0	161	18
6	144	144	0	158	14
	phenyl R-φ-I				
o	142	159	17	171	29
m		152	10	162	20
p		148	6	159	17
o,o		176	34	194	52
m,m		160	18	178	36

the N lone pair to the σ^*(CI) antibonding orbital. This quantity is reported in Table 4 where its variation conforms to

Table 4. NBO Second-Order Perturbation Theory E(2) (Kcal/Mol) for Transfer from the N Lone Pair of NH_3 to the σ^*(C−I) Antibonding Orbital

	H	F	F−H	CN	CN−H
n	alkynes RC−C_n−CI				
0	9.66	10.17	0.51	11.90	2.24
2	10.10	10.00	−0.10	11.55	1.45
4	10.38	10.31	−0.07	11.44	1.06
	alkenes $R_2C-(CH)_n-CHI$				
0	5.41	7.64	2.23	9.06	3.65
2	5.46	5.80	0.34	7.42	1.96
4	5.51	5.57	0.06	6.71	1.20
6	5.57	5.62	0.05	6.51	0.94
	phenyl R-φ-I				
o	5.44	6.54	1.10	7.24	1.80
m		6.04	0.60	6.7	1.26
p		5.83	0.39	6.48	1.04
o,o		7.75	2.31	8.96	3.52
m,m		6.56	1.12	7.80	2.36

the trends of other parameters. E(2) is larger for the alkynes than for the sp^2-hybridized carbons and increases as more triple bonds are added to the chain, with minimal changes accompanying additional double bonds. Cyano substituents exert a more enlarging effect than F atoms, and the effects of the latter die off more quickly with distance from I than those of the former. Partly because of the disubstitution of the alkenes, these chains are more affected than the alkynes by substituents. There is once again a diminishment of the substituent effect as it is moved from ortho to meta to para, and the effects of disubstitution are roughly twice those of monosubstitution.

It is commonly assumed that the strength of a noncovalent bond is heavily influenced by the intensity of the σ-hole on the Lewis acid. This intensity is measured here as the maximum of the molecular electrostatic potential (V_{max}) on an isodensity surface with ρ = 0.001 au. The values contained in Table 5 indicate that a much more intense hole is associated with the alkynes, by roughly a factor of 2. These deeper σ-holes are

Table 5. Intensity of the σ-Hole on the I Atom (V_{max}, Kcal/Mol) on the ρ = 0.001 au Isodensity Surface of the Lewis Acid Monomer

	H	F	F−H	CN	CN−H
n	alkynes RC−C_n−CI				
0	36.3	38.5	2.2	49.5	13.2
2	39.1	38.8	−0.3	48.3	9.2
4	40.6	40.3	−0.3	47.6	7.0
	alkenes $R_2C-(CH)_n-CHI$				
0	17.2	27.4	10.2	39.4	22.2
2	17.6	19.8	2.2	31.8	14.2
4	17.3	17.9	0.6	27.8	10.5
6	17.2	17.8	0.6	26.2	9.0
	phenyl R-φ-I				
o	16.5	20.5	4.0	23.4	6.9
m		20.2	3.7	24.9	8.4
p		19.5	3.0	25.3	8.8
o,o		24.4	7.9	29.7	13.2
m,m		23.9	7.4	32.6	16.1

consistent with the interaction energies that are also about twice as strong for the alkynes. Also consistent is that the elongation of the alkyne enhances V_{max}, with little effect on the alkenes. Substituent effects in the next columns of Table 5 again echo much stronger effects of C≡N vs F and a slowly tapering effect as the substituent is moved further from the I atom. The disubstitution in the alkenes results in a greater σ-hole enhancement than that is observed for the monosubstituted alkynes. There is one interesting distinction of the phenyl data in Table 5. Whereas the energetics and other parameters discussed above diminished in the $o > m > p$ order, the sequence is reversed for the effects of the C≡N group on the I σ-hole, where it is the para-substitution that yields the deepest hole.

Another manifestation of the formation of a XB is the change in the internal covalent bond length of the C−I bond. As may be seen in the first column of Table 6, this bond is stretched when NH_3 interacts with any of the unsubstituted Lewis acids, and this stretch is considerably larger for the alkynes. F-substitution has little effect on the magnitude of this stretching, with only very small magnification. The stretching is

Table 6. Stretch Induced in the Internal r(C−I) Bond (Å) Caused By Complexation with NH_3

	H	F	F−H	CN	CN−H
n	alkynes RC−C_n−CI				
0	0.022	0.025	0.003	0.029	0.007
2	0.023	0.023	0.000	0.028	0.005
4	0.025	0.024	−0.001	0.027	0.002
	alkenes $R_2C-(CH)_n-CHI$				
0	0.006	0.014	0.008	0.014	0.008
2	0.002	0.005	0.003	0.009	0.007
4	0.004	0.004	0.000	0.005	0.001
6	0.004	0.004	0.000	0.005	0.001
	phenyl R-φ-I				
o	0.004	0.009	0.005	0.008	0.004
m		0.005	0.001	0.006	0.002
p		0.005	0.001	0.006	0.002
o,o		0.014	0.010	0.014	0.010
m,m		0.007	0.003	0.009	0.005

https://doi.org/10.1021/acs.jpca.1c03817
J. Phys. Chem. A 2021, 125, 5069−5077

larger for the C≡N substituents, but only slightly larger than that for the unsubstituted species.

Spectroscopic Aspects. One of the most useful experimental indicators of the presence of a H-bond or other noncovalent bonds is associated with the NMR chemical shift undergone by the atoms involved in the bond. The change in the shielding of the I nucleus upon forming each complex listed in Table 7 displays some interesting patterns. In the first place, while the shielding increases when NH_3 is added to the two smaller alkynes, this change is reversed to a strong decrease for the longer HC≡C−C≡C−C≡C−I. The alkene shift changes are all negative but are unusual in that this drop is lowest for $H_2C-(CH)_2-CHI$. The effects of substitutions on the dimerization-induced shielding changes are erratic. Whereas F-substitution on the smallest alkyne increases the shielding, an opposite drop in shielding occurs for the two larger alkynes. The largest drop in shielding is noted when the HC−C≡C−CI is replaced by NC−C−C≡C−CI. These I shielding changes do not seem particularly useful as a general guide.

Table 7. Change in the Chemical Shielding of the I Nucleus (Ppm) Caused By Complexation with NH_3

	H	F	F−H	CN	CN−H
n	alkynes RC−C_n−CI				
0	135.4	148.2	12.8	139.2	3.8
2	218.8	55.8	−163.0	−293.1	−511.9
4	−305.1	−345.1	−40.0	−216.8	88.3
	alkenes $R_2C-(CH)_n-CHI$				
0	−241.9	−89.1	152.8	−47.6	194.3
2	−65.2	−166.0	−100.8	−176	−110.8
4	−108.8	−216.5	−107.7	−247.6	−138.8
6	−170.5	−148.3	22.2	−177.7	−7.2
	phenyl R-φ-I				
o	−27.2	288.0	315.2	195.8	223.0
m		−20.3	6.9	−21.0	6.2
p		4.2	31.4	−29.6	−2.4
o,o		124.4	151.6	140.6	167.8
m,m		−28.3	−1.1	−53.0	−25.8

Much more consistent and potentially useful results are the shielding changes in the N nucleus of the base. Table 8 reveals that complexation with the iodinated acid leads to the deshielding of this atom by approximately 17−29 ppm, and the amount of this deshielding increases as the alkyne or alkene grows longer. Substitution increases the degree of deshielding in all cases, much more so for CN than for F. Also, the effect of substitution is attenuated as the substituent moves further from the XB site, as observed also for the energetics and other properties. There is one small anomaly in that the CN-substitution of the longest alkyne leads to an increase, rather than a decrease, of the N shielding. Nonetheless, there seems to be a strong linear correlation, with coefficient 0.86, between the interaction energy and the shielding of this N nucleus, as exhibited in Figure 3, encompassing all complexes considered here. The slope of this curve is such that each additional 1.7 ppm of deshielding of the N nucleus corresponds to bond strengthening by 1.0 kcal/mol.

Table 8. Change in the Chemical Shielding of the N Nucleus (Ppm) of NH_3 Caused By Complexation with the Lewis Acid

	H	F	F−H	CN	CN−H
n	alkynes RC−C_n−CI				
0	−23.2	−25.2	−2.0	−28.0	−4.8
2	−25.5	−25.7	−0.2	−28.8	−3.3
4	−26.9	−27.4	−0.5	−24.4	2.5
	alkenes $R_2C-(CH)_n-CHI$				
0	−16.6	−22.1	−5.5	−24.2	−7.6
2	−17.4	−18.5	−1.1	−22.0	−4.6
4	−17.7	−19.0	−1.3	−21.9	−4.2
6	−19.4	−20.2	−0.8	−22.5	−3.1
	phenyl R-φ-I				
o	−17.6	−23.1	−5.5	−21.7	−4.1
m		−18.9	−1.3	−20.0	−2.4
p		−18.6	−1.0	−20.6	−3.0
o,o		−23.1	−5.5	−24.8	−7.2
m,m		−20.2	−2.6	−23.1	−5.5

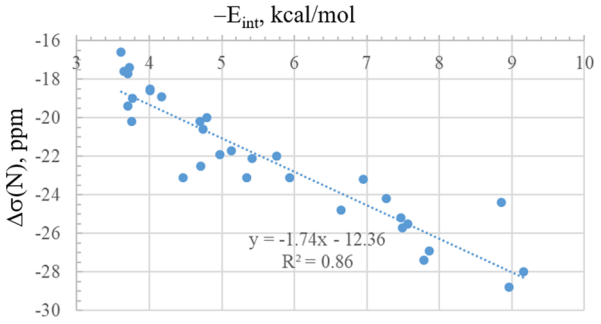

Figure 3. Linear correlation between interaction energies and change in the shielding of the N atom of NH_3 resulting from complexation with Lewis acid

Also of interest would be the shielding of the C atom to which the I is attached. This atom is deshielded by the interaction with NH_3, by approximately 7−17 ppm, as indicated in Table 9. It is most deshielded in the alkynes, less so in the alkenes, and even less in the phenyl group. The effects on its shielding change caused by substitution are generally negative, that is, greater deshielding, and this effect is maximized when the substituent lies closer to the CI bond.

Another spectroscopic parameter that might be considered for a direct correlation with the strength of the XB is the ν(C−

Table 9. Change in the Chemical Shielding of the C Nucleus of the CI Bond (Ppm) Caused By Complexation with NH_3

	H	F	F−H	CN	CN−H
n	alkynes RC−C_n−CI				
0	−12.5	−10.7	1.8	−14.5	−2.0
2	−15.3	−15.6	−0.3	−15.9	−0.6
4	−15.7	−15.8	−0.1	−16.6	−0.9
	alkenes $R_2C-(CH)_n-CHI$				
0	−7.4	−8.7	−1.3	−14.0	−6.6
2	−10.9	−10.9	0.0	−13.7	−2.8
4	−9.8	−9.5	0.3	−11.8	−2.0
6	−9.7	−10.1	−0.4	−13.8	−4.1
	phenyl R-φ-I				
o	−6.7	−7.8	−1.1	−8.5	−1.8
m		−8.1	−1.4	−7.5	−0.8
p		−7.5	−0.8	−8.2	−1.5
o,o		−8.3	−1.6	−9.0	−2.3
m,m		−8.6	−1.9	−9.4	−2.7

https://doi.org/10.1021/acs.jpca.1c03817
J. Phys. Chem. A 2021, 125, 5069−5077

I) stretching frequency. However, an analysis of this type is clouded by the lack of a pure C−I stretching motion, as this displacement is frequently coupled with other intramolecular motions. For example, the C−I stretch in F_2C=CHI is mixed with C−C−F bending; the C−I stretch is coupled with the C−F and C−C stretches in F−C≡C−C≡C−I. Nonetheless, it is possible in most cases to choose a mode which contains at least a large proportion of C−I stretch. With this caveat in mind, Table 10 presents the changes induced in this stretching

Table 10. Change in the CI Stretching Frequency (Cm^{-1}) Caused By Complexation with NH_3

	H	F	F−H	CN	CN−H
n	alkynes RC−C_n−CI				
0	−32.0	−26.4	5.6	−21.1	10.9
2	−20.6	−16.0	4.6	−13.2	7.4
4	−11.6	−9.4	2.2	−11.7	−0.1
	alkenes R_2C−$(CH)_n$−CHI				
0	−11.4	−3.2	8.2	0.7	12.1
2	0.0	0.2	0.2	−1.7	−1.7
4	5.5	−8.3	−13.8	0.0	−5.5
6	2.0	4.6	2.6	−6.6	−8.6
	phenyl R-φ-I				
o	−2.5	5.3	7.8	5.9	8.4
m		2.9	2.9	1.5	1.5
p		−0.3	−0.3	0.2	0.2
o,o		−0.9	−0.9	−3.1	−3.1
m,m		4.2	4.2	3.3	3.3

mode by the introduction of the XB to NH_3. The uppermost section indicates that the XB causes a red shift of this mode to lower frequencies by an amount which diminishes as the alkyne grows longer. The introduction of a substituent reduces the amount of this red shift and by a larger amount for C≡N than that for F. Changes in the alkenes are less clear, but they include a red shift at least for the smallest H_2C=CHI. The coupling of the C−I with other modes in the alkenes leads to similarly complicated effects of substituents. Their effect appears to reduce the red shift for the smallest alkene, with more nuanced trends for the longer ones. With respect to the phenyls in the lowest section of Table 9, the substituent seems to reverse the shift from red to blue. This effect is attenuated as the substituent moves from the ortho and then to the meta and para positions.

DISCUSSION

The effects of elongating the chains are consistent with the standard considerations of electron withdrawal via Hammet constants.[60] Inductive field σ_F and resonance σ_R for each C≡C bond are equal to 0.22 and 0.01, respectively, so the addition of each triply bonded unit is expected to enhance the withdrawal of electrons from the I atom and thus deepen its σ-hole and strengthen the ensuing XB. The negligible effects of the additional double bonds in the alkenes can be reconciled with the small values of the opposite sign of its σ_F and σ_R equal to 0.13 and −0.17, respectively. The more substantial effects of the C≡N substituents vs F are also consonant with σ_F/σ_R, which are 0.51/0.15 for the former and 0.45/−0.39 for the latter. With regard to substituents C≡N and F, it must be emphasized that the alkynes and alkenes were subjected to mono and disubstitution, respectively, so their larger effects upon the alkenes must be viewed through that lens. With that in mind, it should be noted that the disubstitutions within the context of the phenyl rings had much larger effects than monosubstitution, nearly double in fact. Also, in the same line of phenyl substitution, it would appear that proximity to the I is the sole guiding factor, exclusive of resonance considerations, as the effects clearly diminish in the $o > m > p$ sequence.

The effects of the C≡N substituents are fairly strong and diminish slowly as the alkyne or alkene chain grows in length, and the C≡N groups move further from the I atom. Their effects diminish roughly linearly with the reciprocal of the number of intervening C atoms. The increase in this number of atoms from 2 to 6 decreases the effect of the substituent upon the interaction energy by roughly half for the alkynes and by 2/3 for the alkenes, so lingering effects will be exerted continuously even for longer chains. The increase in intervening C atoms between the C≡N and I in the phenyl rings exhibits a somewhat lesser effect on the energetics. The displacement from the ortho to para position reduces its strengthening by only 1/4. Not only is the effect of a fluoro substituent milder than that of cyano, but its effects die off more quickly with distance from I. These changes become negligible for more than 2 intervening atoms in the alkynes and 4 atoms in the disubstituted alkenes. On the other hand, its smaller effects within the phenyl group are appreciable even for the para position.

There has been only modest study to date of halogen bonds formed by unsaturated C−I bonds. The alkynic −C≡C−I group has been considered as the XB donor,[61] particularly with its applications to asymmetric catalysis. When the −C≡C−I group is attached to a phenyl ring,[62] it forms CI··N XBs to a number of different N-bases, with R(I··N) distances in the range of 2.7−3.4 Å, with our computed distances to NH_3 of 2.9−3.1 Å lying square in the middle of that range. The authors found a downfield shift of the acetylenic C of approximately 15−26 ppm, which comports well with our calculated deshielding of 12−17 ppm. Alkenic C−I bonds have been studied as well, as in their XBs with aromatic N-oxides.[63] The placement of EWSs such as $COOCH_3$ on an iodinated alkene has been shown to deepen the σ-holes on I[64] with parallel repercussions for the XB.

Aromatic CI··N XBs have been the subject of a slightly more extensive study, for example, with regard to azobenzenes,[65] 4-iodotetrafluorophenylalanine,[66] C_6F_5I,[67] or the architecture of the crystals formed between ortho-, meta-, or para-diiodotetrafluorobenzene and 2,7-dipyridylfluorene.[68] Also, the ability of these aromatic C−I groups to engage in strong XBs forms the basis of an innovative class of highly selective anion-binding agents currently under development.[69−74] Unsubstituted iodobenzene is capable of forming a CI··N XB with quinuclidine,[75] with a R(C··N) separation of 2.93 Å.

Bauzá et al[33] have verified the stronger electron-withdrawing effect of the cyano vs fluoro substituent in the context of tetrafluoroiodobenzenes. Later calculations by this group[32] verified this same pattern in iodobenzene, where the interaction energy with NH_3 was found to be larger by 0.8 kcal/mol for the para CN vs F-substituted iodobenzene, which compares well with our own difference of 0.7. This group also confirmed our finding that m-substitution increases the interaction more than does the placement of the substituent in the p-position. Consistent with the data presented above for NH_3 as the base, the effects of different positions of an F substituent relative to I on a phenyl ring diminish in the $o > m$

https://doi.org/10.1021/acs.jpca.1c03817
J. Phys. Chem. A 2021, 125, 5069−5077

> p order for NCH as the nucleophile,[76] and the bond strengthening increases as more such F groups are added to the ring, which is a conclusion which was recently echoed by Naghani et al.[77] A similar pattern was noted[78] for SF_5 substituents when halogen bonded to pyridine.

Concomitant with the experimental determination of relevant crystal structures, the theoretical analysis[79] of carboxyl-substituted iodobenzenes verified the ability of this EWS to deepen the σ-hole on I, more so for a larger number of such groups. The downfield shift of the C atom bound to I in an XB observed in the calculations described above has been observed experimentally,[80] and it lies in the 5−27 ppm range, similar to the quantitative shielding changes of our calculations. Another study[81] considered aromatic CI within the context of pyrazoles. The authors found the carbon atom attached to I to be a good reporter group of the presence of an XB. Its measured downfield shifts of 6−7 ppm match closely the computed deshielding found here for iodobenzenes.

CONCLUSIONS

While the elongation of an alkene by additional C═C units has little effect on the ability of a terminal CI group to engage in an XB, there is an increment in the XB strength arising from each addition of a C≡C unit. The placement of electron-withdrawing F and C≡N on the end of the chain opposite from the C−I strengthens the XB, but this effect is ameliorated as the EWS is moved further from I. The consequence of F-substitution is smaller than that of C≡N and extends only for a short distance. The effect of cyano substitution is appreciable even when as many as six C atoms lie between this EWS and the C−I group. The EWS also strengthens the C−I XB when added to iodobenzene, with an effect that diminishes with distance from I: $o > m > p$. The alkenes containing two EWSs on the chain terminus display larger substituent effects than alkynes with only a single such EWS, and the aromatic systems are least sensitive to substitution. These effects on the XB energetics are mirrored in other properties such as the XB length, the electron density of the AIM bond critical point, NBO charge transfer into the σ^*(C−I) antibonding orbital, elongation of the C−I covalent bond, σ-hole depth, and changes in the NMR chemical shielding of the relevant C, I, and N atoms. Of the latter, it is the deshielding of the nucleophile's N atom that is most closely aligned with the energetics.

ASSOCIATED CONTENT

Supporting Information

The Supporting Information is available free of charge at https://pubs.acs.org/doi/10.1021/acs.jpca.1c03817.

Cartesian coordinates of monomers and complexes (PDF)

AUTHOR INFORMATION

Corresponding Author

Steve Scheiner − *Department of Chemistry and Biochemistry, Utah State University, Logan, Utah 84322-0300, United States;* orcid.org/0000-0003-0793-0369; Email: steve.scheiner@usu.edu

Author

Jordan Lapp − *Department of Chemistry and Biochemistry, Utah State University, Logan, Utah 84322-0300, United States*

Complete contact information is available at: https://pubs.acs.org/10.1021/acs.jpca.1c03817

Notes

The authors declare no competing financial interest.

ACKNOWLEDGMENTS

This material is based upon the work supported by the National Science Foundation under Grant No. 1954310.

REFERENCES

(1) Alkorta, I.; Elguero, J.; Frontera, A. Not Only Hydrogen Bonds: Other Noncovalent Interactions. *Cryst.* **2020**, *10*, 180.

(2) Gomila, R. M.; Frontera, A. Charge assisted halogen and pnictogen bonds: insights from the Cambridge Structural Database and DFT calculations. *CrstEngComm* **2020**, *22*, 7162−7169.

(3) Mahmoudi, G.; Abedi, M.; Lawrence, S. E.; Zangrando, E.; Babashkina, M. G.; Klein, A.; Frontera, A.; Safin, D. A. Tetrel Bonding and Other Non-Covalent Interactions Assisted Supramolecular Aggregation in a New Pb(II) Complex of an Isonicotinohydrazide. *Molecules* **2020**, *25*, 4056.

(4) Alkorta, I.; Elguero, J.; Del Bene, J. E.; Mó, O.; Montero-Campillo, M. M.; Yáñez, M. Mutual Influence of Pnicogen Bonds and Beryllium Bonds: Energies and Structures in the Spotlight. *J. Phys. Chem. A* **2020**, *124*, 5871−5878.

(5) Scheiner, S. Understanding noncovalent bonds and their controlling forces. *J. Chem. Phys.* **2020**, *153*, 140901.

(6) Trujillo, C.; Rozas, I.; Elguero, J.; Alkorta, I.; Sánchez-Sanz, G. Modulating intramolecular chalcogen bonds in aromatic (thio)-(seleno)phene-based derivatives. *Phys. Chem. Chem. Phys.* **2019**, *21*, 23645−23650.

(7) Mó, O.; Montero-Campillo, M. M.; Alkorta, I.; Elguero, J.; Yáñez, M. Ternary Complexes Stabilized by Chalcogen and Alkaline-Earth Bonds: Crucial Role of Cooperativity and Secondary Non-covalent Interactions. *Chem. A Eur. J.* **2019**, *25*, 11688−11695.

(8) Del Bene, J. E.; Alkorta, I.; Elguero, J. Exploring N...C tetrel and O...S chalcogen bonds in HN(CH)SX:OCS systems, for X = F, NC, Cl, CN, CCH, and H. *Chem. Phys. Lett.* **2019**, *730*, 466−471.

(9) Mani, D.; The X-C...Y Carbon Bond. In *Noncovalent Forces*, Scheiner, S., Ed. Springer: Heidelberg, 2015, 323−356.

(10) Mani, D.; Arunan, E. The X−C···π (X = F, Cl, Br, CN) Carbon Bond. *J. Phys. Chem. A* **2014**, *118*, 10081−10089.

(11) Yang, Q.; Zhou, B.; Li, Q.; Scheiner, S. Weak σ-Hole Triel Bond between C_5H_5Tr (Tr=B, Al, Ga) and Haloethyne: Substituent and Cooperativity Effects. *ChemPhysChem* **2021**, *22*, 481−487.

(12) Grabowski, S. J. The Nature of Triel Bonds, a Case of B and Al Centres Bonded with Electron Rich Sites. *Molecules* **2020**, *25*, 2703.

(13) Grabowski, S. J. Pnicogen and tetrel bonds—tetrahedral Lewis acid centres. *Struct. Chem.* **2019**, *30*, 1141−1152.

(14) Grabowski, S. J. Tetrel bond−σ-hole bond as a preliminary stage of the S_N2 reaction. *Phys. Chem. Chem. Phys.* **2014**, *16*, 1824−1834.

(15) Scheiner, S. Origins and properties of the tetrel bond. *Phys. Chem. Chem. Phys.* **2021**, *23*, 5702−5717.

(16) Liu, N.; Li, Q.; McDowell, S. A. C. Reliable Comparison of Pnicogen, Chalcogen, and Halogen Bonds in Complexes of 6-OXF2-Fulvene (X = As, Sb, Se, Te, Be, I) With Three Electron Donors. *Front. Chem.* **2020**, *8*, DOI: 10.3389/fchem.2020.608486.

(17) Chandra, S.; Suryaprasad, B.; Ramanathan, N.; Sundararajan, K. Nitrogen as a pnicogen?: evidence for π-hole driven novel pnicogen bonding interactions in nitromethane−ammonia aggregates using matrix isolation infrared spectroscopy and ab initio computations. *Phys. Chem. Chem. Phys.* **2021**, *23*, 6286−6297.

(18) Zhang, L.; Li, D. Theoretical studies on how to tune the π-hole pnicogen bonds by substitution and cooperative effects. *Int. J. Quantum Chem.* **2021**, *121*, e26531.
(19) Echeverría, J. Cooperative Effects between Hydrogen Bonds and C═O···S Interactions in the Crystal Structures of Sulfoxides. *Cryst. Growth Des.* **2021**, *21*, 2481−2487.
(20) Scheiner, S. Relative Strengths of a Pnicogen and a Tetrel Bond and Their Mutual Effects upon One Another. *J. Phys. Chem. A* **2021**, *125*, 2631−2641.
(21) Murray, J. S.; Lane, P.; Clark, T.; Politzer, P. σ-hole bonding: molecules containing group VI atoms. *J. Mol. Model.* **2007**, *13*, 1033−1038.
(22) Hassel, O. Structural aspects of interatomic charge-transfer bonding. *Science* **1970**, *170*, 497−502.
(23) Lommerse, J. P. M.; Stone, A. J.; Taylor, R.; Allen, F. H. The nature and geometry of intermolecular interactions between halogens and oxygen or nitrogen. *J. Am. Chem. Soc.* **1996**, *118*, 3108−3116.
(24) Allen, F. H.; Lommerse, J. P. M.; Hoy, V. J.; Howard, J. A. K.; Desiraju, G. R. Halogen···O(nitro) supramolecular synthon in crystal engineering: A combined crystallographic database and ab initio molecular orbital study. *Acta Cryst.* **1997**, *53*, 1006−1016.
(25) Alkorta, I.; Rozas, S.; Elguero, J. Charge-transfer complexes between dihalogen compounds and electron donors. *J. Phys. Chem. A* **1998**, *102*, 9278−9285.
(26) Farina, A.; Meille, S. V.; Messina, M. T.; Metrangolo, P.; Resnati, G.; Vecchio, G. Resolution of racemic 1,2-dibromohexafluoropropane through halogen -bonded supramolecular helices. *Angew. Chem. Int. Ed. Engl.* **1999**, *38*, 2433−2436.
(27) Clark, T.; Hennemann, M.; Murray, J. S.; Politzer, P. Halogen bonding: the σ-hole. *J. Mol. Model.* **2007**, *13*, 291−296.
(28) Desiraju, G. R.; Ho, P. S.; Kloo, L.; Legon Anthony, C.; Marquardt, R.; Metrangolo, P.; Politzer, P.; Resnati, G.; Rissanen, K. Definition of the halogen bond (IUPAC Recommendations 2013). *Pure Appl. Chem.* **2013**, *85*, 1711−1713.
(29) Grabowski, S. J. Hydrogen and halogen bonds are ruled by the same mechanisms. *Phys. Chem. Chem. Phys.* **2013**, *15*, 7249−7259.
(30) Montero-Campillo, M. M.; Brea, O.; Mó, O.; Alkorta, I.; Elguero, J.; Yáñez, M. Modulating the intrinsic reactivity of molecules through non-covalent interactions. *Phys. Chem. Chem. Phys.* **2019**, *21*, 2222−2233.
(31) Duarte, D. J. R.; Sosa, G. L.; Peruchena, N. M.; Alkorta, I. Halogen bonding. The role of the polarizability of the electron-pair donor. *Phys. Chem. Chem. Phys.* **2016**, *18*, 7300−7309.
(32) Alkorta, I.; Sanchez-Sanz, G.; Elguero, J. Linear free energy relationships in halogen bonds. *Crst. Eng. Comm.* **2013**, *15*, 3178−3186.
(33) Bauzá, A.; Quiñonero, D.; Frontera, A.; Deyà, P. M. Substituent effects in halogen bonding complexes between aromatic donors and acceptors: a comprehensive ab initio study. *Phys. Chem. Chem. Phys.* **2011**, *13*, 20371−20379.
(34) Inscoe, B.; Rathnayake, H.; Mo, Y. Role of Charge Transfer in Halogen Bonding. *J. Phys. Chem. A* **2021**, *125*, 2944−2953.
(35) Ping, N.; Zhang, H.; Meng, L.; Zeng, Y. Insight into the halogen-bonding interactions in the C6F5X···ZH3 (X = Cl, Br, I; Z = N, P, As) and C6F5I···Z (Ph)3 (Z = N, P, As) complexes. *Struct. Chem.* **2021**, *32*, 767−774.
(36) Politzer, P.; Murray, J. S.; Clark, T. Halogen bonding: An electrostatically-driven highly directional noncovalent interaction. *Phys. Chem. Chem. Phys.* **2010**, *12*, 7748−7757.
(37) Riley, K. E.; Murray, J. S.; Fanfrlík, J.; Rezác, J.; Solá, R. J.; Concha, M. C.; Ramos, F. M.; Politzer, P. Halogen bond tunability II: the varying roles of electrostatic and dispersion contributions to attraction in halogen bonds. *J. Mol. Model.* **2013**, *19*, 4651−4659.
(38) Frisch, M. J.; Trucks, G. W.; Schlegel, H. B.; Scuseria, G. E.; Robb, M. A.; Cheeseman, J. R.; Scalmani, G.; Barone, V.; Mennucci, B.; Petersson, G. A., et al. *Gaussian 09, Revision B.01*; Wallingford, CT, 2009.
(39) Feller, D. The role of databases in support of computational chemistry calculations. *J. Comput. Chem.* **1996**, *17*, 1571−1586.
(40) Schuchardt, K. L.; Didier, B. T.; Elsethagen, T.; Sun, L.; Gurumoorthi, V.; Chase, J.; Li, J.; Windus, T. L. Basis Set Exchange: A Community Database for Computational Sciences. *J. Chem. Inf. Model.* **2007**, *47*, 1045−1052.
(41) Yang, J.; Yu, Q.; Yang, F.-L.; Lu, K.; Yan, C.-X.; Dou, W.; Yang, L.; Zhou, P.-P. Competition and cooperativity of hydrogen-bonding and tetrel-bonding interactions involving triethylene diamine (DABCO), H2O and CO2 in air. *New J. Chem.* **2020**, *44*, 2328−2338.
(42) Tondro, T.; Roohi, H. Substituent effects on the halogen and pnictogen bonds characteristics in ternary complexes 4-YPhNH2···PH2F···ClX (Y = H, F, CN, CHO, NH2, CH3, NO2 and OCH3, and X = F, OH, CN, NC, FCC and NO2): A theoretical study. *J. Chem. Sci.* **2020**, *132*, 18.
(43) Scheiner, S. On the capability of metal−halogen groups to participate in halogen bonds. *CrstEngComm* **2019**, *21*, 2875−2883.
(44) Forni, A.; Pieraccini, S.; Franchini, D.; Sironi, M. Assessment of DFT Functionals for QTAIM Topological Analysis of Halogen Bonds with Benzene. *J. Phys. Chem. A* **2016**, *120*, 9071−9080.
(45) Scheiner, S. Differential Binding of Tetrel-Bonding Bipodal Receptors to Monatomic and Polyatomic Anions. *Molecules* **2019**, *24*, 227.
(46) Bauzá, A.; García-Llinás, X.; Frontera, A. Charge-assisted triel bonding interactions in solid state chemistry: A combined computational and crystallographic study. *Chem. Phys. Lett.* **2016**, *666*, 73−78.
(47) Esrafili, M. D.; Vessally, E. A theoretical evidence for cooperative enhancement in aerogen-bonding interactions: Open-chain clusters of $KrOF_2$ and $XeOF_2$. *Chem. Phys. Lett.* **2016**, *662*, 80−85.
(48) Mardirossian, N.; Head-Gordon, M. How Accurate Are the Minnesota Density Functionals for Noncovalent Interactions, Isomerization Energies, Thermochemistry, and Barrier Heights Involving Molecules Composed of Main-Group Elements? *J. Chem. Theory Comput.* **2016**, *12*, 4303−4325.
(49) Boys, S. F.; Bernardi, F. The calculation of small molecular interactions by the differences of separate total energies Some procedures with reduced errors. *Mol. Phys.* **1970**, *19*, 553−566.
(50) Latajka, Z.; Scheiner, S. Primary and secondary basis set superposition error at the SCF and MP2 levels: H_3N–Li^+ and H_2O–Li^+. *J. Chem. Phys.* **1987**, *87*, 1194−1204.
(51) Boese, A. D.; Jansen, G.; Torheyden, M.; Höfener, S.; Klopper, W. Effects of counterpoise correction and basis set extrapolation on the MP2 geometries of hydrogen bonded dimers of ammonia, water, and hydrogen fluoride. *Phys. Chem. Chem. Phys.* **2011**, *13*, 1230−1238.
(52) Bader, R. F. W.; Carroll, M. T.; Cheeseman, J. R.; Chang, C. Properties of atoms in molecules: atomic volumes. *J. Am. Chem. Soc.* **1987**, *109*, 7968−7979.
(53) Bader, R. F. W. *Atoms in Molecules, A Quantum Theory*; Clarendon Press: Oxford, 1990; *22*, 438.
(54) Keith, T. A. *AIMAll*, TK Gristmill Software: Overland Park KS, 2013.
(55) Lu, T.; Chen, F. Multiwfn: A multifunctional wavefunction analyzer. *J. Comput. Chem.* **2012**, *33*, 580−592.
(56) Noro, T.; Sekiya, M.; Koga, T. Segmented contracted basis sets for atoms H through Xe: Sapporo-(DK)-nZP sets (n = D, T, Q). *Theor. Chem. Acc.* **2012**, *131*, 1124.
(57) Noro, T.; Sekiya, M.; Koga, T. Sapporo-(DKH3)-nZP (n = D, T, Q) sets for the sixth period s-, d-, and p-block atoms. *Theor. Chem. Acc.* **2013**, *132*, 13.
(58) Kar, T.; Scheiner, S. Comparison of cooperativity in CH··O and OH··O hydrogen bonds. *J. Phys. Chem. A* **2004**, *108*, 9161−9168.
(59) Scheiner, S.; Nagle, J. F. Ab initio molecular orbital estimates of charge partitioning between Bjerrum and ionic defects in ice. *J. Phys. Chem.* **1983**, *87*, 4267−4272.
(60) Hansch, C.; Leo, A.; Taft, R. W. A survey of Hammett substituent constants and resonance and field parameters. *Chem. Rev.* **1991**, *91*, 165−195.
(61) Mamane, V.; Peluso, P.; Aubert, E.; Weiss, R.; Wenger, E.; Cossu, S.; Pale, P. Disubstituted Ferrocenyl Iodo- and Chalcoge-

https://doi.org/10.1021/acs.jpca.1c03817
J. Phys. Chem. A 2021, 125, 5069−5077

noalkynes as Chiral Halogen and Chalcogen Bond Donors. *Organometallics* **2020**, *39*, 3936−3950.
(62) Szell, P. M. J.; Dragon, J.; Zablotny, S.; Harrigan, S. R.; Gabidullin, B.; Bryce, D. L. Mechanochemistry and cocrystallization of 3-iodoethynylbenzoic acid with nitrogen-containing heterocycles: concurrent halogen and hydrogen bonding. *New J. Chem.* **2018**, *42*, 10493−10501.
(63) Truong, K.-N.; Rautiainen, J. M.; Rissanen, K.; Puttreddy, R. The C−I···$^{-}$O−N^{+} Halogen Bonds with Tetraiodoethylene and Aromatic N-Oxides. *Cryst. Growth Des.* **2020**, *20*, 5330−5337.
(64) Yuan, Y.; Mills, M. J. L.; Li, F.; Du, Y.; Wei, J.; Su, W. Halogen bonds and other noncovalent interactions in the crystal structures of trans-1,2-diiodo alkenes: an ab initio and QTAIM study. *J. Mol. Model.* **2020**, *26*, 331.
(65) Virkki, M.; Maurice, A.; Forni, A.; Sironi, M.; Dichiarante, V.; Brevet, P.-F.; Metrangolo, P.; Kauranen, M.; Priimagi, A. On the molecular optical nonlinearity of halogen-bond-forming azobenzenes. *Phys. Chem. Chem. Phys.* **2018**, *20*, 28810−28817.
(66) Bergamaschi, G.; Lascialfari, L.; Pizzi, A.; Martinez Espinoza, M. I.; Demitri, N.; Milani, A.; Gori, A.; Metrangolo, P. A halogen bond-donor amino acid for organocatalysis in water. *Chem. Commun.* **2018**, *54*, 10718−10721.
(67) Wang, W.; Zhang, Y.; Wang, Y.-B. The $\pi\cdots\pi$ stacking interactions between homogeneous dimers of $C_6F_xI_{(6-x)}$ (x = 0, 1, 2, 3, 4, and 5): A comparative study with the halogen bond. *J. Phys. Chem. A* **2012**, *116*, 12486−12491.
(68) Grosu, I. G.; Pop, L.; Miclăuş, M.; Hădade, N. D.; Terec, A.; Bende, A.; Socaci, C.; Barboiu, M.; Grosu, I. Halogen Bonds (N—I) at Work: Supramolecular Catemeric Architectures of 2,7-Dipyridyl-fluorene with ortho-, meta-, or para-Diiodotetrafluorobenzene Isomers. *Cryst. Growth Des.* **2020**, *20*, 3429−3441.
(69) Ostler, F.; Piekarski, D. G.; Danelzik, T.; Taylor, M. S.; García Mancheño, O. Neutral Chiral Tetrakis-Iodo-Triazole Halogen-Bond Donor for Chiral Recognition and Enantioselective Catalysis. *Chem. A Eur. J.* **2021**, *27*, 2315−2320.
(70) Pancholi, J.; Beer, P. D. Halogen bonding motifs for anion recognition. *Coord. Chem. Rev.* **2020**, *416*, No. 213281.
(71) Decato, D. A.; Riel, A. M. S.; Berryman, O. B. Anion Influence on the Packing of 1,3-Bis(4-Ethynyl-3-Iodopyridinium)-Benzene Halogen Bond Receptors. *Cryst.* **2019**, *9*, 522.
(72) Bunchuay, T.; Docker, A.; Martinez-Martinez, A. J.; Beer, P. D. A Potent Halogen-Bonding Donor Motif for Anion Recognition and Anion Template Mechanical Bond Synthesis. *Angew. Chem. Int. Ed.* **2019**, *58*, 13823−13827.
(73) Borissov, A.; Marques, I.; Lim, J. Y. C.; Félix, V.; Smith, M. D.; Beer, P. D. Anion Recognition in Water by Charge-Neutral Halogen and Chalcogen Bonding Foldamer Receptors. *J. Am. Chem. Soc.* **2019**, *141*, 4119−4129.
(74) Klein, H. A.; Beer, P. D. Iodide Discrimination by Tetra-Iodotriazole Halogen Bonding Interlocked Hosts. *Chem. A Eur. J.* **2019**, *25*, 3125−3130.
(75) Otte, F.; Kleinheider, J.; Hiller, W.; Wang, R.; Englert, U.; Strohmann, C. Weak yet Decisive: Molecular Halogen Bond and Competing Weak Interactions of Iodobenzene and Quinuclidine. *J. Am. Chem. Soc.* **2021**, *143*, 4133−4137.
(76) Tang, Q.; Li, Q. Non-additivity of F substituent in enhancing the halogen bond in $C_6H_5I\cdots NCH$. *Comput. Theor. Chem.* **2015**, *1070*, 21−26.
(77) Naghani, F. F.; Emamian, S.; Zare, K. Exploring influence of fluorine substitution on the strength and nature of halogen bond between iodobenzene and hydrogen cyanide. *J. Phys. Org. Chem.* **2021**, e4213.
(78) Sumii, Y.; Sasaki, K.; Tsuzuki, S.; Shibata, N. Studies of Halogen Bonding Induced by Pentafluorosulfanyl Aryl Iodides: A Potential Group of Halogen Bond Donors in a Rational Drug Design. *Molecules* **2019**, *24*, 3610.
(79) Chernysheva, M. V.; Bulatova, M.; Ding, X.; Haukka, M. Influence of Substituents in the Aromatic Ring on the Strength of Halogen Bonding in Iodobenzene Derivatives. *Cryst. Growth Des.* **2020**, *20*, 7197−7210.
(80) Szell, P. M. J.; Cavallo, G.; Terraneo, G.; Metrangolo, P.; Gabidullin, B.; Bryce, D. L. Comparing the Halogen Bond to the Hydrogen Bond by Solid-State NMR Spectroscopy: Anion Coordinated Dimers from 2- and 3-Iodoethynylpyridine Salts. *Chem. A Eur. J.* **2018**, *24*, 11364−11376.
(81) Popa, M. M.; Man, I. C.; Draghici, C.; Shova, S.; Caira, M. R.; Dumitrascu, F.; Dumitrescu, D. Halogen bonding in 5-iodo-1-arylpyrazoles investigated in the solid state and predicted by solution 13C-NMR spectroscopy. *CrstEngComm* **2019**, *21*, 7085−7093.

https://doi.org/10.1021/acs.jpca.1c03817
J. Phys. Chem. A 2021, 125, 5069−5077